

PERFORMANCE VALIDATION OF THE CALTECH DUCTED-FAN AT A FIXED OPERATING POINT

Kyong Lim*, Marc Trotoux†, John Doyle‡
 Control and Dynamical System, Caltech

Abstract

Using measured input and output data and *a priori* assumptions on nominal model and a linear fractional transformation uncertainty structure, a family of model validating uncertainty sets are constructed for robust control analysis and design of the Caltech ducted fan. Based on an identified uncertainty set, the predicted closed loop performance for any given controller is compared to the directly measured performance. This paper reports current status of the ongoing work at Caltech and more results will likely be reported at the conference.

1 Introduction

In general, an "optimal" robust performance controller [1] is defined with respect to a set of plants having a specific LFT uncertainty structure. A key premise in the above notion is that the LFT uncertainty structure and the corresponding uncertainty bound is known. In applications however, particularly for systems which are more complex, the issue of selecting a suitable uncertainty structure and their bounds is not trivial. Subsequently, it is difficult to predict worst case performance, and much less attain "optimal" robust performance. The current popularity of μ analysis and less of μ synthesis is a testament to this state of practice in control engineering. To cope with this reality, many approaches have been proposed in the past (a sample given in [2],[3]) which builds on classical model validation ideas to explicitly include unknown but bounded model uncertainties in addition to unknown exogenous noise.

In this study, we investigate issues directly related to the performance validation of the Caltech ducted fan test article. Since both multivariable robust control and identification theories assume linear, time-invariance, the operation of the ducted fan undergoing horizontal flight at a trim point is considered. First, based on a nominal model which is obtained from first principles and parameter identification, and a chosen uncertainty structure, the corresponding parametrized set of all model validating uncertainty set is obtained using a closed loop extension of the approach outlined in [3]. Among this parametrized model validating set, we consider a smallest weighted model validating uncertainty set for the given uncertainty structure for the ducted fan. Second, the uncertainty model is evaluated by comparing its predicted closed loop worst case performance to the measured worst case closed loop performance for any controller that is closed loop stable when implemented.

*Research Engineer, visiting from NASA Langley Research Center, lim@cds.caltech.edu

†Research Engineer, visiting from Aerospatiale, France, trotoux@cds.caltech.edu

‡Professor, doyle@cds.caltech.edu

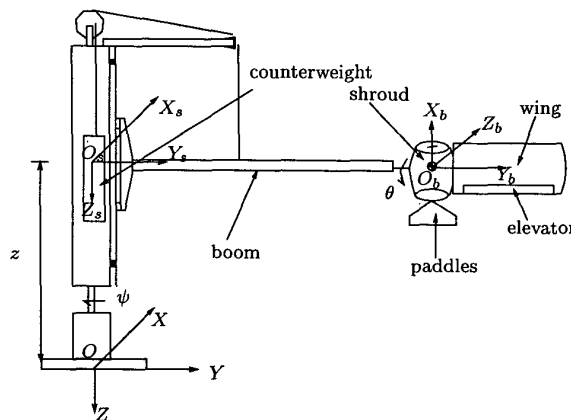


Figure 1: Ducted Fan Body

2 Caltech Ducted Fan Model

2.1 Equations of Motion

A schematic of the Ducted Fan is described in Figure 1 and Figure 2. $(0, X, Y, Z)$ is an inertial coordinate system, (O_s, X_s, Y_s, Z_s) a stand center of mass, body fixed coordinate system, (O_b, X_b, Y_b, Z_b) a shroud center of mass, body fixed coordinate system, and (O_w, X_w, Y_w, Z_w) the wind coordinate system. ψ is the angle between $[OX]$ and the projection of $[O_s X_s]$ on the plane (XOY) , θ , the pitch axis angle i.e. the angle between the local horizontal $[O_s X_s]$ and the $[O_b X_b]$ axis and z the algebraic distance OO_s . The airspeed at the center of mass of the ducted-fan (shroud+wing+boom) is denoted by $V_s = \frac{\dot{\psi}}{r_s}$, the angle of attack by α_s , the flight path angle by γ_s , the paddle angle by δ_p , the elevator angle by δ_e and the motor voltage by V_m . Subscripts s and w denote variables related to shroud and wing respectively.

The Lagrange's equations of motion are given by

$$I_Z^s \ddot{\psi} = -r_s F_{X_s}^s - r_w F_{X_s}^w - r_b F_{X_s}^b - \dot{\theta} I_{X_b}^p \Omega \cos \theta \quad (1)$$

$$(m_b + m_f + \frac{m_c}{r^2}) \ddot{z} = mg + F_{Z_s}^s + F_{Z_s}^w + F_{Z_s}^b \quad (2)$$

$$I_{Y_b, r}^f \ddot{\theta} = M_{Y_s}^s + M_{Y_s}^w + I_{X_b}^p \psi \Omega \cos \theta \quad (3)$$

where I_Z^s is the moment of inertia of the fan, boom and counterweight about OZ ; $I_{Y_b, r}^f$, the moment of inertia of the fan about $O_b Y_b$ when wing in rearward position; $I_{X_b}^p$,

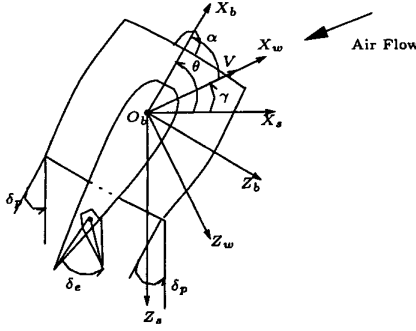


Figure 2: Shroud and Wing Conventions

the moment of inertia of the propeller and the motor about $O_b X_b$; $F_{X_s}^b$, the X_s component of the boom aerodynamic force; $F_{X_s}^w$ and $F_{Z_s}^w$, the X_s and Z_s components of the wing aerodynamic force; $M_{Y_s}^w$, the Y_s component of the wing aerodynamic moment; $F_{X_s}^s$ and $F_{Z_s}^s$, the X_s and Z_s components of the shroud aerodynamic force; $M_{Y_s}^s$, the Y_s component of the shroud aerodynamic moment; r_b , the effective moment arm for the boom; r_w , the effective moment arm for the wing; r_s , the distance between O_b and the plane XOZ ; m_b the mass of the boom; m_c , the mass of the counterweight; m_f , the mass of the fan; r , the pulley gear ratio; g , the gravity and Ω the motor velocity; $m := m_b + m_f - \frac{m_c}{r}$.

Boom and wing aerodynamics Due to the rotation of the fan, the wing will experience increasing velocities from its root. A similar situation occurs for the boom. The aerodynamic forces of the wing and boom may be written as:

$$F_{X_s}^b = F_{X_s}^b(\psi, \dot{z}, C_{D_b})$$

$$F_{X_s}^w = F_{X_s}^w(\psi, \dot{z}, C_D^w, C_L^w)$$

$$F_{Z_s}^w = F_{Z_s}^w(\psi, \dot{z}, C_D^w, C_L^w)$$

$$M_{Y_s}^w = M_{Y_s}^w(\psi, \dot{z}, C_M^w, C_D^w, C_L^w)$$

where C_{D_b} is the drag coefficient of the boom (cylinder) and C_D^w , C_L^w and C_M^w , determined by a series of wind tunnel tests, are functions of α_w and δ_e . For now, the effects of all other derivatives are assumed negligible.

Shroud Forces and Moments There are two contributions to the shroud aerodynamic forces and moments: the thrust from the ducted fan engine and the aerodynamic forces of the shroud. In order to determine the shroud forces $F_{X_s}^s$ and $F_{Z_s}^s$, and moment $M_{Y_s}^s$, four 2-D table lookup ($F_{X_s}^s$, C_D^s , C_L^s and C_M^s) as a function of α_s , V_m or δ_p are necessary.

Motor Speed A 2-D table lookup, function of V_m and δ_p , will be used to determine the motor velocity Ω . The effects of V and α are neglected.

For now, the actuators are assumed to be perfect and the moments of inertias of the fan (shroud and wing) and the propeller about ($O_b X_b$) and ($O_b Z_b$) are neglected.

2.2 Linearization about Trim

The ducted fan is described by a set of ODEs $\dot{x} = f(x, u)$ where $x^T = [\psi, z, \dot{z}, \theta, \dot{\theta}]$ and $u^T = [V_m, \delta_p, \delta_e]$. f is derived from the equations 1, 2 and 3. The navigation variable, z , is necessary to control the altitude during experiments since the vertical movement is constrained by the testbed. Figure 3 is a schematic of the linearization about a trim point. By solving the non-linear algebraic equa-

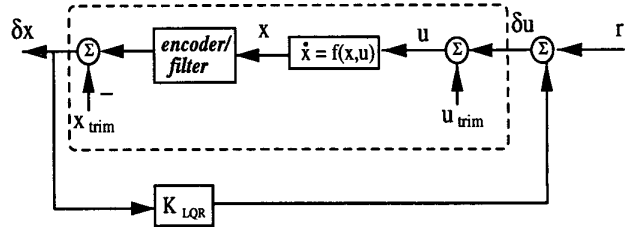


Figure 3: Linear motion about trim for Ducted fan.

tions for the forward flight at constant velocity, altitude and pitch angle, we obtain the trim conditions consisting of the pitch angle θ , the motor voltage V_m , the paddle angle δ_p and the elevator angle δ_e . The trim condition corresponds to the following conditions:

$$x_{trim}^T = [\psi_o, 0, 0, \theta_{trim}, 0],$$

and

$$u_{trim}^T = [V_{m_{trim}}, \delta_{p_{trim}}, \delta_{e_{trim}}] / f(x_{trim}, u_{trim}) = 0_{1 \times 5}$$

At a specified ψ_o , a linearized fifth order model is obtained by computing the Jacobian of f at this trim point. It turns out that the above trim point (at a tangent velocity of $V_s = 8 \text{ m/sec}$) is unstable and a stabilizing Linear Quadratic Regulator is required. Since the encoders directly measure ψ , z and θ , a second order filter is used in each channel to estimate the corresponding velocities.

3 Performance Validation

Our main goal in this study is to obtain a set of plants which satisfies a priori assumptions and is also consistent with input/output measurement data. Of course the end goal is to be able to predict or attain closed loop performance more reliably in practice. We begin by summarizing recent results in model validation and uncertainty model parameterization.

3.1 Control Objective

Consider a robust regulation problem in the sense of minimizing the weighted H_∞ norm from the disturbances, r , at all three plant inputs to the outputs under model uncertainties. The control inputs are V_m , δ_p and δ_e and the measured variables are ψ , z and θ . Of course a wide range of controllers can result depending strongly on the control engineer. In particular, this wide range of controllers for this single physical plant can result due to basic differences in a priori assumptions on the models and exogenous noise and disturbances.

we select weights W which is a measure of relative uncertainty sizes desired. We then seek at each frequency the smallest x such that \mathcal{D}_{xw} is model validating, as follows:

$$\min_{\psi, \phi, \delta_1, \dots, \delta_{n_p}, x}$$

subject to $\delta_i \in \mathcal{F}_i \quad i = 1, \dots, n_p$

$$\xi_i = \delta_i \eta_i, \quad i = 1, \dots, n_p$$

$$|\delta_i| - |w_i| \leq 0, \quad i = 1, \dots, n_p$$

$$\|\xi_i\| - x |w_i| \|\eta_i\| \leq 0, \quad i = n_p + 1, \dots, \tau$$

$$x \geq 0$$

$$\|\phi\| \leq b_o$$

where n_p is the number of uncertain real parameters.

4 Results

Consider a trim point corresponding to horizontal flight of $V_s = 8m/sec$ at which a linearized state-space (analytical) model is obtained of order five. This model has the inputs $(V_m, \delta_e, \delta_p)$ and the outputs $(\psi, z, \dot{z}, \theta, \dot{\theta})$. The results of four cases are reported in this paper. First two cases are based purely on simulation wherein the true model and measurement noise is assumed known. Satisfactory results in the first two cases is necessary in order to consider case 3 where a nominal plant is obtained from a system identification algorithm based on measured input-output data, and case 4 where the analytical model was enhanced via an ad-hoc parameter identification procedure based on measurement data.

4.1 Measurement Data, Nominal Model

In cases 1 and 2, a linearized analytical model is chosen as the true model. In case 1, the true model is taken as the nominal model. This is a necessary test case where if the noise allowance is sufficiently large (at least as large as the true noise) then the identified model error should be zero. To simulate a nominal model for case 2, the true model is perturbed at all five plant outputs by $\Delta_{true} = [.3 \ .1 \ -.05 \ .2 \ -.1]$, with no perturbations in Δ_{add} and eigenvalues. Using this true model, a Linear Quadratic regulator controller is designed. Figure 6 show the true (simulated) versus the nominal closed loop maximum singular value of the transfer function matrices where a significant difference is noted. A Schroder-phased signal is used as the test input signal, r , for the closed loop system. In cases 1 and 2, the assumed measurement noise allowance is set to the maximum noise, i.e.,

$$V_{noise} = \max_{\omega} \|\text{FFT}[y_{noise}(t)]\|_2 * I_{5 \times 5}$$

In case 3, a state-space identification algorithm is used to obtain a 10th order model such that it is unstable open loop but stable when closed with the LQR controller which was used to collect measurement data. In case 4, an analytically based fifth-order model was adjusted via parameter identification. A least squares procedure was used to minimize nominal closed loop output error.

4.2 Uncertainty Model

Figure 7 shows the interconnection structure of the nominal and assumed structured uncertainty. Uncertainties in

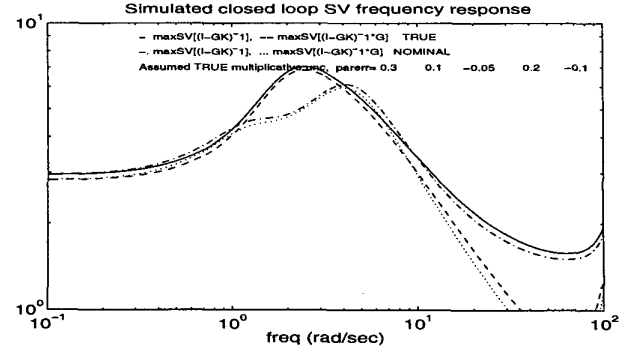


Figure 6: True vs Nominal closed loop frequency response, case 2

the plant eigenvalues, output multiplicative uncertainties and additive uncertainty from V_m to ψ is considered.

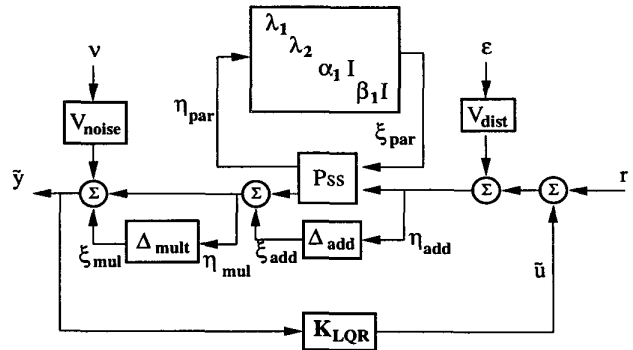


Figure 7: Interconnection Structure

Figures 8 and 9 show the identified multiplicative uncertainty for cases 1 and 2 respectively. The following uncertainty weights were used in the optimization: $w_{eval} = 0_{5 \times 5}$, $w_{mult} = I_{5 \times 5}$, and $w_{add} = .001$. To de-emphasize the use of additive uncertainty from V_m to ψ , a small value of $w_{add} = .001$ was used in the optimization. Within computational accuracy and reliability, Figure 8 shows that zero multiplicative uncertainty is almost recovered. On the other hand, for case 2, the identified multiplicative uncertainties resembles the true values, Δ_{true} , in Figure 9.

Figure 10 shows a representative comparison of the closed loop response of the measured output variable θ versus the response predicted by the identified nominal model in case 3.

Figure 11 shows the identified multiplicative and additive uncertainty for case 3. The following uncertainty weights were used in the optimization: $w_{eval} = .02 * I_{10 \times 10}$, $w_{mult} = I_{5 \times 5}$, and $w_{add} = 1$. This means that the real and imaginary z-plane eigenvalues of the identified plant were allowed to be any value within a square box of length .04 about each of the 4 complex conjugate nominal eigenvalues and an abscissa range of .04 for 2 purely real nominal eigenvalues. In addition, the relative importance of the additive and multiplicative uncertainties are equal. Figure 11 shows the five multiplicative uncertainty and the single additive uncer-

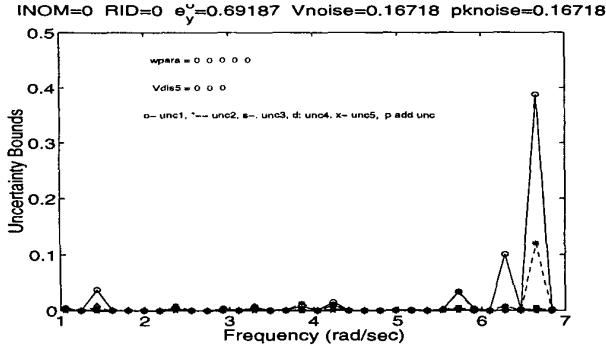


Figure 8: Identified multiplicative uncertainty for case 1

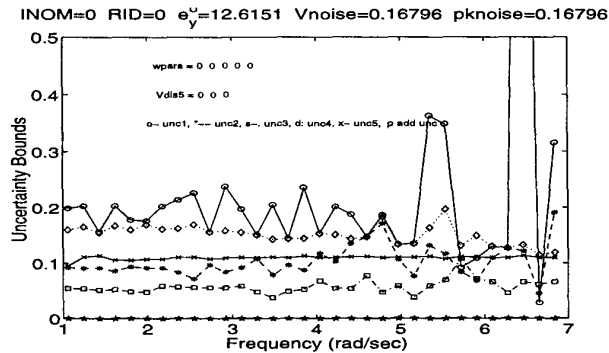


Figure 9: Identified multiplicative uncertainty for case 2

tainty computed. Note that there is a large uncertainty around $.5Hz$ which could have been caused by unmodeled dynamics in the form of boom fixture flexibility and the periodic excitation of the wake due to nonuniform test walls surrounding the rotating ducted fan.

Figure 12 shows the identified multiplicative/additive uncertainty for case 4. The same uncertainty weights, W as in case 3 was used in the optimization.

In summary, the identified model validating uncertainty models appeared too large for controller analysis and design applications. The predicted nominal closed loop response is significantly different from the measured outputs (typical of figure 10). Hence, we are currently investigating ways to improve our nominal models since a too large nominal error will almost guarantee a correspondingly large uncertainty set.

References

- [1] Stein, G., and Doyle, J.C., "Beyond singular values and loopshapes," *AIAA Journal of Guidance, Control, and Dynamics*, Vol. 14, pp. 5-16, 1991.
- [2] Special Issue on System Identification and Control, *IEEE Transactions on Automatic Control*, v.37, n.7, pp. 899-1008, July 1992.
- [3] Lim, K.B., and Giesy, D.P., "Parameterization of model validating uncertainty models for controller optimizations," *1998 AIAA GNC conference*, Boston, MA, August 1998.

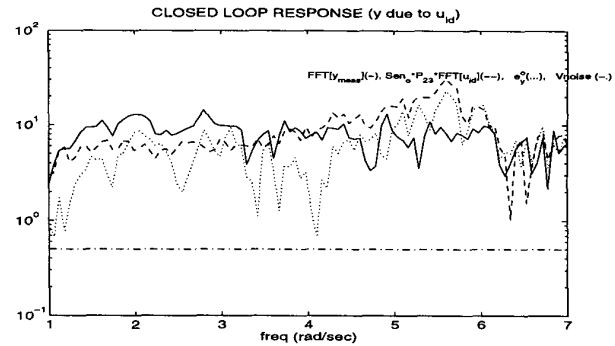


Figure 10: Comparison of measured vs nominal closed loop response for θ , case 3

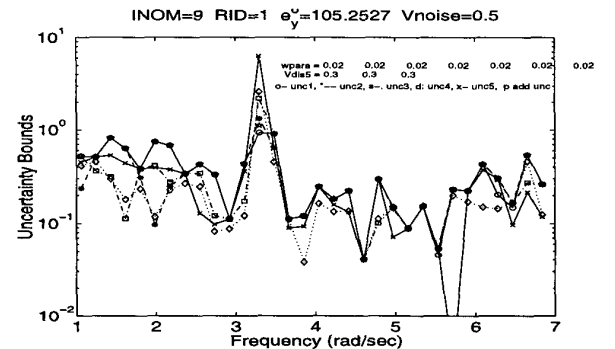


Figure 11: Identified multiplicative/additive uncertainty for case 3

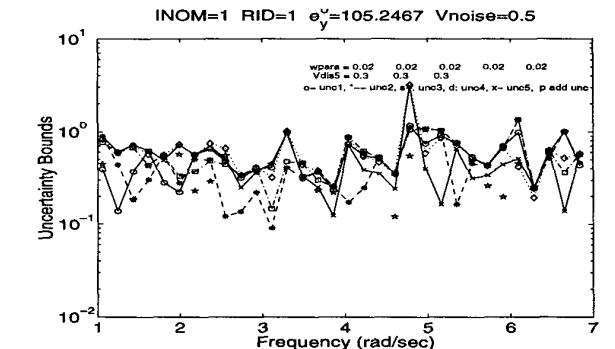


Figure 12: Identified multiplicative/additive uncertainty for case 4